Received: 24 February 2023 | Revised: 10 July 2023 | Accepted: 11 July 2023

DOI: 10.1002/dta.3555

RESEARCH ARTICLE

WILEY

In vitro cannabinoid receptor activity, metabolism, and detection in seized samples of CH-PIATA, a new indole-3-acetamide synthetic cannabinoid

Caitlyn Norman[1] | Marie H. Deventer[2] | Olivia Dremann[3] | Robert Reid[1] | Katleen Van Uytfanghe[2] | Claude Guillou[4] | Inge M. J. Vinckier[5] | Niamh Nic Daéid[1] | Alex Krotulski[6] | Christophe P. Stove[2]

[1]Leverhulme Research Centre for Forensic Science, School of Science and Engineering, University of Dundee, Dundee, UK

[2]Laboratory of Toxicology, Department of Bioanalysis, Faculty of Pharmaceutical Sciences, Ghent University, Ghent, Belgium

[3]College of Arts and Sciences, Arcadia University, Glenside, Pennsylvania, USA

[4]European Commission, Joint Research Centre (JRC), Ispra, Italy

[5]Laboratory of Customs and Excises, Vilvoorde, Belgium

[6]Center for Forensic Science Research and Education, Frederic Rieders Family Foundation, Willow Grove, Pennsylvania, USA

Correspondence
Caitlyn Norman, Leverhulme Research Centre for Forensic Science, School of Science and Engineering, University of Dundee, Dundee, UK.
Email: cynorman@dundee.ac.uk

Funding information
Fonds Wetenschappelijk Onderzoek, Grant/Award Number: 1S54521N; Leverhulme Trust, Grant/Award Number: RC-2015-01; National Institute of Justice, Grant/Award Number: 2020-DQ-BX-0007; Scottish Prison Service

Abstract

The rapidly evolving synthetic cannabinoid receptor agonist (SCRA) market poses significant challenges for forensic scientists. Since the enactment of a generic ban in China, a variety of new compounds have emerged capable of evading the legislation by carrying new structural features. One recent example of a SCRA with new linker and head moieties is CH-PIATA (CH-PIACA, CHX-PIATA, CHX-PIACA). CH-PIATA bears an additional methylene spacer in the linker moiety between the indole core and the traditional carbonyl component of the linker. This study describes detections in 2022 of this new SCRA in the United States, Belgium, and Scottish prisons. CH-PIATA was detected once in a seized powder by Belgian customs and 12 times in Scottish prisons in infused papers or resin. The metabolites of CH-PIATA were investigated via in vitro human liver microsome (HLM) incubations and eight metabolites were identified, dominated by oxidative biotransformations. A blood sample from the United States was confirmed to contain a mixture of SCRAs including CH-PIATA via presence of the parent and at least five of the metabolites identified from HLM incubations. Furthermore, this paper evaluates the intrinsic in vitro cannabinoid 1 and 2 (CB_1 and CB_2) receptor activation potential of CH-PIATA reference material and the powder seized by Belgian customs by means of β-arrestin 2 recruitment assays. Both the reference and the seized powder showed a weak activity at both CB receptors with signs of antagonism found. Based on these results, the expected harm potential of this newly emerging substance remains limited.

KEYWORDS
bioassay, forensic toxicology, metabolism, new psychoactive substances, synthetic cannabinoid receptor agonists

1 | INTRODUCTION

Synthetic cannabinoid receptor agonists (SCRAs) are the largest class of new psychoactive substances (NPS) with over 220 individual compounds monitored by the European Monitoring Centre for Drugs and Drug Addiction (EMCDDA).[1] These compounds bind to the cannabinoid 1 and 2 (CB_1 and CB_2) receptors and are designed to mimic the effects of Δ^9-tetrahydrocannabinol (Δ^9-THC), the main psychoactive component of cannabis.[2–6] However, SCRAs are often significantly more potent than Δ^9-THC[7–9] and can have adverse effects more closely related to psychostimulants, such as methamphetamine, or opioids, such as fentanyl, than cannabis. These adverse effects include chest pain, acute kidney injury, stroke, rhabdomyolysis, and death.[10–12]

The illicit market for SCRAs is constantly evolving, often in response to national and international legislation, particularly in producer countries, such as China.[2,13] China typically controlled one SCRA at a time; however, in July 2021, China enacted analog controls for SCRAs based on distinct structural components, which covered all of the most prevalent compounds on the market at the time.[14,15] This includes the *tert*-leucinate- and valinate-indole- and indazole-3-carboxamide SCRAs, which were historically among the most potent.[8,16–18] Following the enactment of these analog controls, new structural scaffolds that circumvent the new controls emerged or re-emerged, including the monocyclic pyrazole (e.g., 5F-3,5-AB-PFUPPYCA),[19] oxoindolin (e.g., BZO-POXIZID),[15] brominated core (e.g. ADB-5′Br-INACA),[20,21] and acetamide linker (e.g., ADB-FUBIATA), which have an additional methylene in the linker moiety of the structure.[22,23]

A new SCRA with an acetamide linker that has recently emerged is CH-PIATA (*N*-cyclohexyl-2-(1-pentylindol-3-yl)acetamide), also known as CH-PIACA, CHX-PIATA, and CHX-PIACA (Figure 1). CH-PIATA was first notified in Europe by the EU Early Warning System on March 24, 2022, following detection in seizures of beige powder by Spanish Customs on February 1, 2022 and State Police in Germany on March 12, 2022.[24] CH-PIATA was also detected in a sample of beige powder seized on February 1, 2022, by the Danish Customs Agency.[25] It was first reported in the United States on April 29, 2022, following detection in an herbal material sample submitted to the laboratory on November 11, 2021, seemingly the first occurrence worldwide.[26] Additionally in the Unites States, the Drug Enforcement Administration's (DEA's) National Forensic Laboratory Information System (NFLIS) first reported CH-PIATA in Q2 2022.[27]

To date, there have not been any reported detections of CH-PIATA in biological samples. This may be due to SCRAs being heavily metabolized so the parent compound is often not found in biological fluids, particularly urine.[28,29] It is therefore relevant to identify putative metabolites of CH-PIATA. Several approaches to determine SCRA metabolism are available, including in vitro, in silico, in vivo, in zebrafish, and using the fungus *Cunninghamella elegans*, with human hepatocyte incubation being recommended over human liver microsome (HLM) incubation. However, HLM incubation is the most popular in vitro metabolism model, likely because it is a much more affordable and simple method compared with hepatocyte incubation.[30]

Furthermore, the pharmacological properties of CH-PIATA, such as its cannabinoid receptor activation potential, are currently unknown. To assess this, two live cell- and activity-based bioassays were employed, monitoring the recruitment of the intracellular protein β-arrestin2 (βarr2) to the ligand-activated receptor (CB_1 and CB_2 receptor). The assays are based on the NanoLuc Binary Technology (NanoBiT®, Promega), which employs the concept of functional complementation. In short, the CB_1 or CB_2 receptors are fused to an inactive subunit of a split nanoluciferase enzyme, whereas the other complementary subunit is linked to βarr2, an intracellular signaling protein that is recruited to the receptor upon activation. This brings both subunits in close proximity and results in functional complementation of the enzyme and restoration of its activity. Upon addition of its substrate furimazine, a luminescent signal is generated, which can be measured using a standard luminometer.

While these βarr2 assays were initially developed to serve as a new screening strategy to detect the presence of cannabimimetic substances

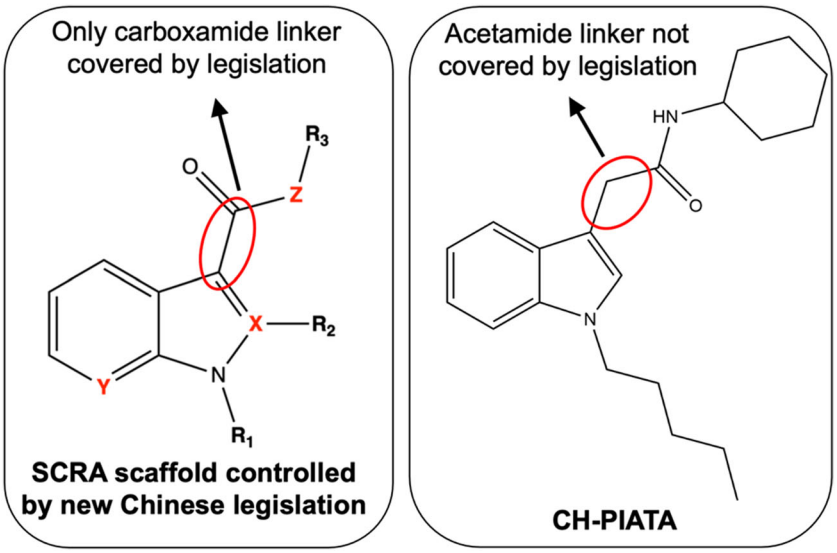

FIGURE 1 Comparison between the SCRA scaffold controlled by the new Chinese analog controls and the chemical structure of CH-PIATA with an acetamide linker (additional methylene between the core and amide). X represents a C or N atom, Y represents N or CH, and Z represents either O, NH, or no atom. R_1 represents an unsubstituted or substituted: C_3–C_8 hydrocarbyl group, heterocyclic group containing 1–3 heteroatoms, or methyl or ethyl group substituted by a heterocyclic group containing 1–3 heteroatoms. R_2 represents a hydrogen atom, methyl group, or no atom. R_3 represents an unsubstituted or substituted: C_6–C_{10} aryl group, C_3–C_{10} hydrocarbyl group, heterocyclic group containing 1–3 heteroatoms, or a methyl or ethyl group substituted by a heterocyclic group containing 1–3 heteroatoms. [Colour figure can be viewed at wileyonlinelibrary.com]

in biological matrices,[31–33] they also serve as excellent tools to investigate the pharmacology of these compounds. Moreover, given the convenience of the stable cell system and the easily applicable protocol, without the need for highly sophisticated equipment or specialized expertise, these assays provide an effective and straightforward way to obtain insights in the characteristics of (new) substances.

This paper reports the detection of CH-PIATA in seized samples in Belgium and prisons in Scotland. The in vitro metabolic fate of CH-PIATA was studied using incubation with HLMs and the identified metabolites were used to confirm the presence of CH-PIATA in a blood sample from the United States. The in vitro intrinsic CB_1 and CB_2 receptor activation potential of CH-PIATA was also evaluated using an activity-based NanoBiT® bioassay.

2 | MATERIALS AND METHODS

2.1 | Materials

2.1.1 | Seized sample analysis (Dundee, UK)

Methanol (LC-MS grade) and water (LC-MS grade) were purchased from Fisher Scientific, UK; bupivacaine and formic acid were obtained from Sigma-Aldrich (Poole, UK). The CH-PIATA reference standard (97.5% purity) was obtained from Chiron AS (Trondheim, Norway). ADB-BUTINACA (>98% purity) and MDMB-4en-PINACA (98.6% purity) were synthesized and supplied by the Sutcliffe Group at Manchester Metropolitan University, Manchester, UK as described previously.[34,35]

2.1.2 | Seized sample analysis (Belgian customs, European Commission, and Ghent Laboratory of Toxicology)

For Fourier transform infrared spectroscopy (FTIR), no solvents or reagents were used. For gas chromatography coupled to mass spectrometry (GC-MS), methanol (LC-MS grade) was obtained from Supelco (Lichrosolv Reag. Ph. Eur. Methanol). DMSO-d_6 solvent was obtained from Sigma-Aldrich (Milan, Italy). For liquid chromatography coupled to time-of-flight mass spectrometry (LC-QTOF-MS), LC-MS grade methanol and formic acid were procured from Chem-Lab NV (Zedelgem, Belgium). Acetonitrile was purchased from Biosolve (Valkenswaard, The Netherlands) and ammonium formate was from Sigma-Aldrich (Diegem, Belgium).

2.1.3 | Metabolism studies (CFSRE, US)

All materials and reagents used for liquid chromatography mass spectrometry (LC-MS) analyses were of LC-MS grade purity. Solvents were purchased from Honeywell Chemicals (Charlotte, NC, USA). The CH-PIATA reference material (purity ≥98%) was purchased from Cayman Chemical (Ann Arbor, MI, USA) and prepared at 1 mg/mL in acetonitrile. Ammonium formate (99%) was purchased from Alfa Aesar (Ward Hill, MA, USA). Formic acid ampoules (1 mL) were purchased from Thermo Fisher Scientific (Waltham, MA, USA). Pooled HLMs were purchased from Thermo Fisher Scientific correlating to 50 donors and pooled at 20 mg/mL. Sodium phosphate dibasic (anhydrous), sodium phosphate monobasic (monohydrate), and magnesium chloride hexahydrate were purchased from VWR (Radnor, USA, PA). Nicotinamide adenine dinucleotide phosphate (NADPH) was purchased from Cayman Chemical.

2.1.4 | Detection in toxicological samples (CFSRE, USA)

The blood sample stemmed from a police case of suspected drug intoxication. It was collected in October 2022 in the state of Indiana. The internal standard used was a 10 ng/mL solution of JWH-018-D9, AKB-48-D9, AB-FUBINACA-D4, XLR-11-D5, ADB-PINACA-D9, and ADBICA-D9 purchased from Cayman Chemical. All other materials and solvents used were from the same sources as detailed in Section 2.1.3.

2.1.5 | Determination of in vitro CB_1 and CB_2 receptor activity

Dulbecco's modified Eagle's medium (DMEM) (GlutaMAX™), Opti-MEM I Reduced Serum, penicillin, streptomycin, and amphotericin B were procured from Thermo Fisher Scientific (Waltham, MA, USA). Fetal bovine serum (FBS) and poly-D-lysine were purchased from Sigma-Aldrich (Darmstadt, Germany). The Nano-Glo® Live Cell reagent and the Nano-Glo® LCS Dilution buffer were obtained from Promega (Madison, WI, USA). Methanol, used for the preparation of the stock solutions, was procured from Chem-Lab NV (Zedelgem, Belgium). CP55,940 was purchased from Sigma-Aldrich, JWH-018 was from LGC (Wesel, Germany), and the reference standards of CH-PIATA (purity ≥98%) and ADB-FUBIATA (purity ≥98%) were kindly provided by Cayman Chemical (Ann, Arbor, MI, USA). The Laboratory of Customs and Excise (Vilvoorde, Belgium) provided a sample of a seized powder containing CH-PIATA.

2.2 | Methods

2.2.1 | Seized sample analysis (Dundee, UK)

The extraction of SCRAs from infused papers and cards and analysis by GC-MS has been described previously. In brief, 2×1 cm^2 pieces from opposite corners of paper samples were extracted in 0.5 mL of 0.25 mg/mL bupivacaine in methanol by ultrasonication (5 min). For resinous materials, 10 mg of the material was extracted in 1 mL of 0.25 mg/mL bupivacaine in methanol using a benchtop vortex (1 min).

GC-MS analysis of sample extracts was performed using a 7820A gas chromatograph coupled to a 5977E mass spectrometer (Agilent technologies, Santa Clara, CA, USA). Injection mode: 1-μL sample

injection was used with a 20:1 split into a 4-mm internal diameter deactivated glass liner pre-packed with quartz wool, injection port temperature: 200°C, carrier gas: He, flow: 1 mL/min. Column: HP-5MS, 0.33 µm, 0.2 mm × 25 m (Agilent Technologies). GC oven: 80°C held for 3 min; 40°C/min to 300°C held for 11 min; total run time: 22.5 min; transfer line: 295°C. The mass spectrometer operated in electron ionization (EI) mode. Ionization conditions: 70 eV in full scan mode (50–550 amu), ion source: 230°C, quadrupole: 150°C. Compound identification by GC-MS criteria has been described previously.

2.2.2 | Seized sample analysis (Belgian customs, European Commission, and Ghent Laboratory of Toxicology)

FTIR

Analysis was performed on the powder without prior sample preparation using an Alpha-FTIR instrument from Bruker (Billerica, MA, US) equipped with an attenuated total reflection (ATR) unit. Twenty-four scans were recorded in the 400–4000 cm^{-1} wave number range, with a resolution of 4 cm^{-1}.

GC-MS

The powder was dissolved in methanol and a small aliquot was used for analysis. Measurements were performed using a Shimadzu® GCMS-QP2010 Ultra (Shimadzu Corporation, Kyoto, JP). Injection mode: 0.5-µL sample injection was used with a 20:1 split, injection port temperature: 280°C, carrier gas: He. Column: DB5-MS (phenyl arylene polymer stationary phase), 0.25 µm, 0.25 mm × 30 m (Agilent J&W). GC oven: 100°C; 15°C/min to 320°C held for 15.33 min; total run time: 30 min; transfer line: 280°C. The mass spectrometer operated in EI mode. Ion source: 200°C.

LC-QTOF-MS

High-resolution mass spectrometry (HRMS) was performed on an aliquot (dissolved in methanol) as described before.[15,36,37] Chromatographic separation was achieved using an Agilent 1290 Infinity LC system, equipped with a Phenomenex Kinetex C_{18}-column (2.6 µM, 3 × 50 mm), maintained at 30°C. The HRMS system used was a 5600+ QTOF with an electrospray ionization (ESI) source (Sciex) and Analyst TF 1.7.1 software, from the same provider. TOF-MS full scan spectra combined with data dependent acquisition of product ion spectra were obtained.

2.2.3 | Nuclear magnetic resonance spectroscopy (NMR)

Nineteen milligrams of the seized CH-PIATA powder was dissolved in 600 µL of deuterated solvent for preparation of the NMR tube. NMR analyses were performed as previously described.[38] NMR spectra were acquired on a Bruker (Rheinstetten, Germany) spectrometer Avance II HD 600 (nominal proton frequency 600.13 MHz), equipped with a 5-mm QCI cryo-probe (^{1}H, ^{13}C, ^{15}N, and ^{19}F), in DMSO-d_6 solvent at 300 K. ^{1}H and ^{13}C NMR chemical shifts are expressed in δ scale (ppm) and referenced to the solvent (DMSO-d_6) residuals, at 2.50 ppm and 39.51 ppm, respectively. The seized powder was characterized by one-dimensional ^{1}H, ^{13}C, ^{19}F and APT, as well as $^{1}H/^{1}H$ COSY, $^{1}H/^{1}H$ TOCSY, $^{1}H/^{13}C$ HMBC, and $^{15}N/^{1}H$ HMBC experiments. Full NMR data (including 2D NMR COSY, TOCSY and HMBC spectra) can be provided in electronic format upon request.

2.2.4 | Metabolism experiments (CFSRE, USA)

CH-PIATA reference standard (50 µL) was dried to completion at 35°C and subsequently reconstituted with 50 µL of phosphate buffer and acetonitrile (50:50, v:v). The reconstituted CH-PIATA (5 µL) was combined with varying combinations of phosphate buffer, HLMs, and/or NADPH: 595-µL buffer in sample A; 570-µL buffer and 25-µL NADPH in sample B; and 520-µL buffer, 50-µL HLMs, and 25-µL NADPH in sample C. This incubation process was performed over 3 days and sample C was prepared in duplicate. Prepared samples were incubated in a water bath (37°C) for 2 h. Following incubation, acetonitrile (500 µL) was added to all samples to stop the metabolic reactions. Samples were then transferred to microcentrifuge tubes and centrifuged (10,000 rpm). The supernatant was transferred to a new test tube and the samples were partially dried at 35°C for 20 min to remove most of the organic solvent in the samples. The supernatant was transferred to a Costar® Spin-X® (Corning Inc., Corning, NY, USA) microcentrifuge tube with a microfilter to remove any remaining cellular material or debris. The resulting sample was transferred to an autosampler vial for analysis by LC-QTOF-MS.

Samples were analyzed on a SCIEX TripleTOF® 5600+ QTOF (Ontario, Canada) coupled with a Shimadzu Nexera XR UHPLC (Kyoto, Japan). Ammonium formate (10 mM, pH 3) and methanol:acetonitrile (50:50) were used as the mobile phase in a linear gradient (95:5 to 5:95) with a flow rate of 0.4 mL/min. A Phenomenex® Kinetex C_{18} analytical column (2.6 µm, 50 mm × 3.0 mm) was used to achieve chromatographic separation of the metabolites. The total analysis run time was 15.5 min. Mass acquisition was performed using data dependent acquisition (information dependent acquisition: IDA). Positive electrospray ionization was used for ionization. Precursor ions were acquired by a TOF MS scan ranging from 100 to 1000 *m/z*. Precursor ions were subsequently filtered in the quadrupole (Q1) using traditional unit mass isolation. Following this filtration, precursor ions were fragmented in the collision cell using a collision energy spread of 35 ± 15 eV and acquired by a TOF MSMS scan ranging from 40 to 1000 m/z. Datafiles were processed using MetabolitePilot™ (SCIEX, Version, 2.0), MasterView™ (SCIEX, Version 1.1), and PeakView® (SCIEX, Version 2.2).

2.2.5 | Detection in toxicological samples (CFSRE, USA)

Blood samples (0.5 mL) were prepared by liquid–liquid extraction. Samples were fortified with 50-µL internal standard (10 ng/mL), followed by addition of 1 mL phosphoric acid in water (5%, v:v) and 3 mL of

extraction solvent (80:10:10 hexane:ethyl acetate: MTBE, v:v). Sample mixtures were rotated for 15 min prior to centrifugation at 4600 rpm for 10 min. The supernatant was then removed and transferred for dry down under nitrogen at 35°C using a Biotage TurboVap evaporator (Uppsala, Sweden). Samples were reconstituted in 200 µL of 10:90 A:B where A was 0.1% formic acid in water and B was 0.1% formic acid in acetonitrile.

Similar to the metabolism experiments, samples were analyzed on a SCIEX TripleTOF® 5600+ QTOF (Ontario, Canada) coupled with a Shimadzu Nexera XR UHPLC (Kyoto, Japan). LC setpoints (e.g., mobile phase, stationary phase) remained the same. The total analysis run time was 15.5 min. Mass acquisition was performed using data independent acquisition (SWATH®). Positive electrospray ionization was used for ionization. Precursor ions were acquired by a TOF MS scan ranging from 100 to 550 m/z. Precursor ions were subsequently filtered in the quadrupole (Q1) using SWATH® acquisition for windowed ($n = 27$) mass isolation. Following this filtration, precursor ions were fragmented in the collision cell using a collision energy spread of 35 ± 15 eV and acquired by a TOF MSMS scan ranging from 40 to 550 m/z. Datafiles were processed using MasterView™ (SCIEX, Version 1.1) and PeakView® (SCIEX, Version 2.2).

2.2.6 | In vitro activity (Ghent University, Belgium)

Intrinsic activation potential at CB_1 and CB_2 receptors of both the CH-PIATA reference standard and a seized powder (Belgian customs) was evaluated using live cell βarr2 recruitment assays, as described before.[31–33] In short, human embryonic kidney (HEK) 293T cells with stable expression of either the CB_1-βarr2 or CB_2-βarr2 system were routinely maintained under a humidified atmosphere at 37°C and 5% CO_2 and were cultured in DMEM (GlutaMAX™) supplemented with 10% heat-inactivated FBS, penicillin (100 IU/mL), streptomycin (100 µg/mL), and amphotericin B (0.25 µg/mL). On the day prior to the assay, cells were trypsinized and seeded in white poly-D-lysine coated 96-well plates at 5×10^4 cells/well, followed by overnight incubation. The next day, cells were rinsed twice with Opti-MEM before adding 100 µL of this medium to each well. Next, the Nano-Glo® Live Cell Reagent, containing the furimazine substrate, was diluted 20-fold in Nano-Glo® LCS Dilution buffer and 25 µL of this mix was added to each well. Subsequently, the plate was placed into a TriStar[2] 942 Multimode Microplate Reader (Berthold Technologies GmbH & Co., Germany) and luminescence was monitored for 10–15 min during an initial equilibration phase. Upon stabilization of the luminescence signal, 10 µL of a 13.5× concentrated test solution was added, followed by a final 2-h luminescence measurement. Test solutions were prepared by serial dilution in Opti-MEM containing 50% MeOH and used within 24 h. A concentration range of CP55,940 was run on every plate and served as a reference compound for further normalization of the generated data. JWH-018 and ADB-FUBIATA were included for comparison with earlier work[9,22,39,40] and appropriate solvent controls were included on every plate. All compounds were analyzed in duplicate in a minimum of three independent experiments ($n \geq 3$). To investigate a potential antagonistic behavior exerted by CH-PIATA, cells (both CB_1-βarr2 or CB_2-βarr2) were pre-treated for 5 min with solvent control or 10 µM of CH-PIATA (13.5× concentrated) after initial equilibration in the system. Subsequently, following a protocol employed for past experiments,[22] 10 nM (CB_1 receptor) or 100 nM (CB_2 receptor) of JWH-018 (14.5× concentrated) was added and luminescence was measured for 2 h.

Raw luminescence signals were corrected for *inter-well* variability in Microsoft Excel 2019, using data from the initial equilibration run, followed by calculation of the area under the curve (AUC). Signals were then blank corrected by subtracting the mean AUC of the solvent controls and the obtained values were used to generate concentration–response curves using the GraphPad Prism software (Version 9.3.0) (San Diego, CA, USA) via fitting the data to a nonlinear regression model (three-parametric logistic fit). Pharmacological parameters EC_{50} (a measure for a substance's potency) and E_{max} (a measure for relative efficacy, representing the maximal obtained effect) were calculated based on the obtained curves. Data were normalized to the E_{max} of CP55,940, arbitrarily set at 100%. AUC values from the highest concentrations were excluded in case of a signal reduction of 20% or more compared with the next (lower) dilution, as this may imply some form of solubility issue or cell toxicity at these high concentrations. The Grubbs test was used to screen for potential outliers, leading to the omission of 2 data points from the complete dataset (420 points) (p value <0.05). For the antagonist experiments, signals from solvent-treated cells were compared with those from CH-PIATA-treated cells, using the nonparametric Mann–Whitney *U* test in GraphPad Prism.

3 | RESULTS AND DISCUSSION

3.1 | Detection in seized samples

Between February 2 and November 23, 2022, CH-PIATA was detected 12 times in five out of 15 Scottish prisons. Data and further information on each sample can be found in the Supporting Information (S1). All samples were infused paper apart from two samples that were incorporated into a resinous material found to be low-THC, high-CBD resin (see Figure 2). In addition to CH-PIATA, four of the infused paper samples contained another SCRA, either MDMB-4en-PINACA ($n = 2$) or ADB-BUTINACA ($n = 2$), and one of the resin samples also contained ADB-BUTINACA. One paper also contained low levels of heroin (6-MAM, paracetamol, and caffeine), although this was likely due to cross-contamination from the handling or storage of multiple drugs by prisoners rather than purposeful addition.

In March 2022, the Belgian customs seized a powder from a suspect package being shipped to Moldova. The identity of the seized powder was confirmed to be CH-PIATA following FTIR, GC-MS, HRMS and NMR analysis. Data and more information can be found in Supporting Information (S2–S5). Some impurities were also found; however, despite substantial efforts, unequivocal identification of these impurities was not possible. Combined, several analyses indicated the presence of CH-IATA (i.e., CH-PIATA analog lacking the pentyl tail) in the seized powder, although compounds with structures

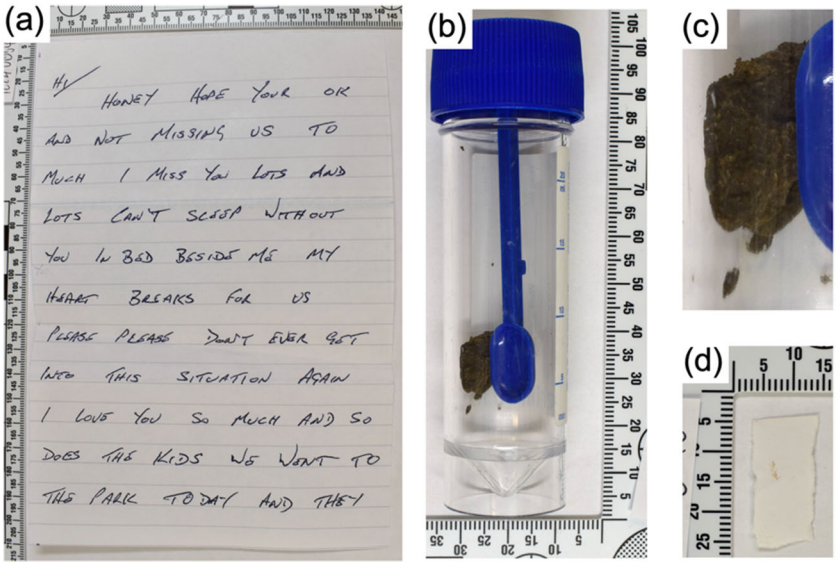

FIGURE 2 Examples of samples seized from the Scottish prisons: (a) paper seized on April 27, 2022, found to contain CH-PIATA and MDMB-4en-PINACA; (b) resinous material seized on May 9, 2022, found to be high-CBD, low-THC resin with CH-PIATA; (c) zoom-in of the resinous material in (b); and (d) paper seized on February 2, 2022, found to contain CH-PIATA.

TABLE 1 CH-PIATA metabolites with biotransformation; molecular formula; retention times; exact masses of the protonated molecules; mass errors; peak areas; and major fragment ions. Metabolites are ordered from most to least abundant across both incubations.

Met #	Biotransformation	Formula	RT (min)	Exact mass $[M+H]^+$ (m/z)	Error (ppm)	Peak area ($\times 10^5$)	Major fragment ions
Parent	CH-PIATA	$C_{21}H_{30}N_2O$	10.15	327.2422	−2.6	792	83, 100, 130, 144, 200, 245
M1	MonoOH (*n*-pentyl tail)	$C_{21}H_{30}N_2O_2$	8.27	343.2364	−4.6	39.8	69, 100, 130, 144, 216, 261, 325
M2	Carboxylation (*n*-pentyl tail)	$C_{21}H_{28}N_2O_3$	7.69	357.2172	−0.2	4.59	85, 100, 230, 258, 339
M3	*N*-dealkylation + MonoOH (indole)	$C_{16}H_{20}N_2O_2$	6.82	273.1599	0.6	4.25	100, 128, 146, 173
M4	MonoOH (indole/acetamide)	$C_{21}H_{30}N_2O_2$	8.76	343.2380	−0.1	4.19	100, 160, 216, 240, 261
M5	DiOH (indole/acetamide)	$C_{21}H_{30}N_2O_3$	8.11	359.2324	−1.5	3.53	100, 134, 162, 218, 232, 259
M6	DiOH (indole/acetamide + *n*-pentyl tail)	$C_{21}H_{30}N_2O_3$	6.99	359.2327	−0.5	2.77	100, 146, 200, 214, 232, 341
M7	MonoOH (cyclohexyl)	$C_{21}H_{30}N_2O_2$	8.53	343.2367	−3.8	1.26	116, 130, 200, 225, 240
M8	*N*-dealkylation	$C_{16}H_{20}N_2O$	7.33	257.1651	0.9	1.21	55, 100, 130, 175

similar to more conventional SCRAs (JWH-type) seemed to be present. Extensive analytical experiments, including fractionation experiments to enrich the impurities, would be needed to allow the complete analytical characterization of the seized sample; however, this lies beyond the scope of the current paper. Overall, combining findings from multiple analytical techniques, the presence of CH-PIATA (approximately 80 molar %) could be concluded, together with several other SCRAs or SCRA precursors (including CH-IATA).

3.2 | Metabolism

Following incubation with HLMs, eight metabolites (M1–M8) were identified for CH-PIATA. The identified metabolites are listed in Table 1 with the molecular formulas, exact masses, retention times, mass errors, peak areas, and diagnostic fragment ions. The metabolites are numbered according to their total peak area, from the highest to the lowest area. Although this does not necessarily reflect a metabolite's abundance (as for example ionization efficiencies may differ between compounds), it is referred to as "abundance" below for simplicity. Proposed structures of the metabolites are organized in a suggested metabolic pathway in Figure 3. The mass spectra of the parent compound and all metabolites can be found in the Supporting Information (S6).

The metabolites eluted between 6.82 and 8.76 min with the parent compound eluting the latest at 10.15 min. The observed biotransformations included hydroxylations, carboxylation, and *N*-dealkylation in various combinations. The most abundant metabolite (M1) had a

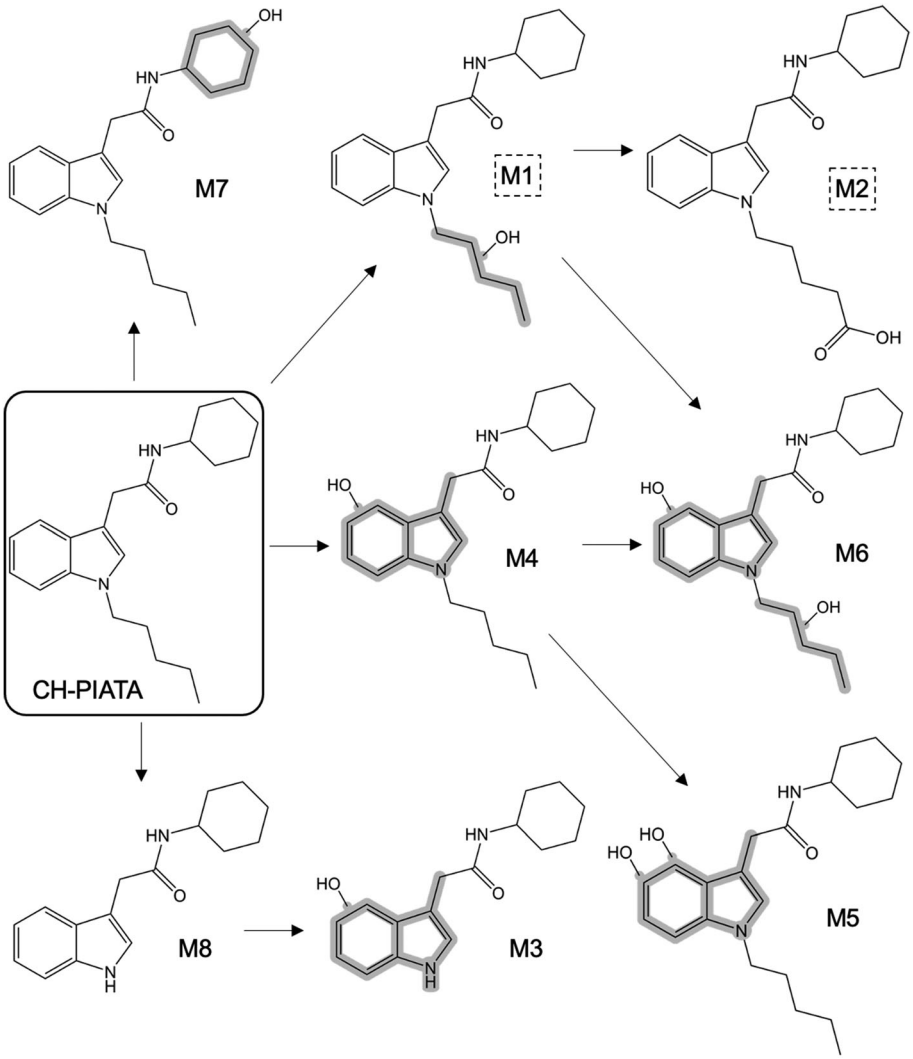

FIGURE 3 Proposed metabolic pathways of CH-PIATA following in vitro incubation with HLMs. Metabolites in dashed line boxes are suggested as suitable urinary markers for toxicological identification.

monohydroxylation (monoOH) at the pentyl tail (e.g., 5-OH-CH-PIATA) and the second most abundant metabolite (M2) had a carboxylation at the pentyl tail (e.g., CH-PIATA *N*-pentanoic acid). The next four most abundant metabolites had biotransformations at the indole core or acetamide linker including monoOH at the indole core in combination with dealkylation (cleavage of the pentyl tail) (M3); monoOH at the indole core or acetamide linker (M4); dihydroxylation (diOH) at the indole core or acetamide linker (M5); and diOH with a monoOH at the indole core or acetamide linker in combination with a monoOH at the pentyl tail (M6). The least abundant metabolites had a monoOH at the cyclohexyl head moiety (M7) and dealkylation (M8).

It should be noted that there are several possible sites of hydroxylation for each of the four main structural components of the SCRA molecule and as such, multiple isomeric hydroxylated metabolites could appear that are not distinguishable with this analysis alone (e.g., 3-OH-CH-PIATA vs. 4-OH-CH-PIATA vs. 5-OH-CH-PIATA, etc., for M1). This holds true for all metabolites with a hydroxylation (M1 and M3–M7) and the molecules are denoted as such in Figure 3.

The metabolite with dealkylation (M8) is the tail-less analog of CH-PIATA, CH-IATA, which has been detected in seized samples as notified by the EU Early Warning System on August 17, 2022.[41] In addition, as the metabolism of CH-IATA has yet to be examined, the metabolite with depentylation in combination with monoOH at the indole core (M3) may also be a metabolite of CH-IATA. This indicates that the presence of either of these metabolites (M3 and M8) in biological fluids could be indicative of the use of either CH-PIATA or CH-IATA, so additional metabolites would be required in order to unequivocally confirm the compound used. This should be further explored through the study of the in vitro metabolism of CH-IATA.

Based on this in vitro data, to identify consumption of this newly emerged SCRA, it is recommended that the parent compound (after β-glucosidase treatment), metabolite M1 with monoOH at the pentyl tail (e.g., 5-OH-CH-PIATA), and metabolite M2 with carboxylation at the pentyl tail (CH-PIATA *N*-pentanoic acid) may be suitable urinary markers for CH-PIATA. It is important to note that the metabolites obtained from incubation with HLMs do not always or necessarily

reflect the metabolites found in biological samples, particularly urine, because HLMs do not contain the enzymes responsible for phase II metabolism. However, the majority of SCRA metabolites have been found to involve only phase I biotransformations. In addition, phase II biotransformations are most prevalent for SCRAs with halogenated tails and good agreement has been found in the metabolites for SCRAs without halogenated tails obtained from incubation with HLMs and human hepatocytes and in human urine and blood.[30,42,43] The recommendation of metabolites M1 and M2 as potentially suitable urinary markers for CH-PIATA is not only based on them being the most abundant metabolites identified from the incubation with HLMs but also that they are two of the most commonly observed metabolites for most pentyl tail-containing SCRAs (e.g., AB-PINACA, Cumyl-PICA, 5F-MDMB-PICA, etc.) in both in vitro data obtained from HLMs and hepatocytes and in vivo data.[44–46]

3.3 | Detection in toxicological samples

CH-PIATA was detected in a blood sample received on 27th October 2022 from Indiana in the United States along with a mixture of other SCRAs: ADB-BUTINACA and one of its metabolites with mono-hydroxylation at the *n*-butyl tail moiety, 4-OH-ADB-BUTINACA[35,47,48]; ADB-INACA, the tail-less analog of ADB-BUTINACA; and MDMB-4en-PINACA and its metabolite with ester hydrolysis, MDMB-4en-PINACA 3,3-dimethylbutanoic acid.[43,49] For the detection of CH-PIATA, the parent was the most abundant (peak area: 5586) but five of the metabolites identified from incubation with HLMs were also detected: M1 (peak area: 3174), M2 (peak area: 1304), M8 (peak area: 590), M5, and M6. M4 and M7 may have also been present as there were small peaks for their masses; however, the fragment data for these metabolites was either poor or not detected. M3 was determined to be not present at detectable levels in this one blood sample.

Although the metabolites differ in their relative abundance, the detection of the CH-PIATA metabolites in the blood sample shows good correspondence with the metabolites identified from incubation with HLMs.

3.4 | In vitro activity

In vitro functional characterization of CH-PIATA was done using two live cell-based bioassays, monitoring the βarr2 recruitment to either the activated CB_1 or CB_2 receptor. Concentration–response curves are depicted in Figure 4 and show a comparison of the activation profiles obtained for the reference standard and the seized sample. Table 2 shows the accompanying pharmacological parameters (EC_{50} and E_{max}).

For the reference standard CP55,940, EC_{50} values of 0.11 (at CB_1) and 0.08 nM (at CB_2) were found, which were slightly lower than previously reported data.[22] Overall, CH-PIATA showed weak receptor activation potential at both CB receptors. A plateau of maximal activation could not be reached for the reference standard of CH-PIATA, thereby precluding the calculation of accurate EC_{50} values. At both CB receptors, a maximal receptor activation of less than 10% (relative to CP55,940) was observed at the highest concentration of 1 μM. Given the pronounced rightward shift of the concentration response curves compared with the reference, the potency of CH-PIATA is predicted to be low. To put this into perspective, the CB_1 receptor relative efficacy and potency found for prototypical SCRA JWH-018 were 348% and 13.4 nM, respectively, in line with earlier reported data.[15,19,22] At the CB_2 receptor, an E_{max} of 76.6% and an EC_{50} value of 3.23 nM was found. Based on these results, the estimated threat to a user of CH-PIATA can be considered low.

At the CB_1 receptor, CH-PIATA was clearly demonstrated to be substantially less active than ADB-FUBIATA, a substance which can be considered the first emerging acetamide SCRA (for comparison,

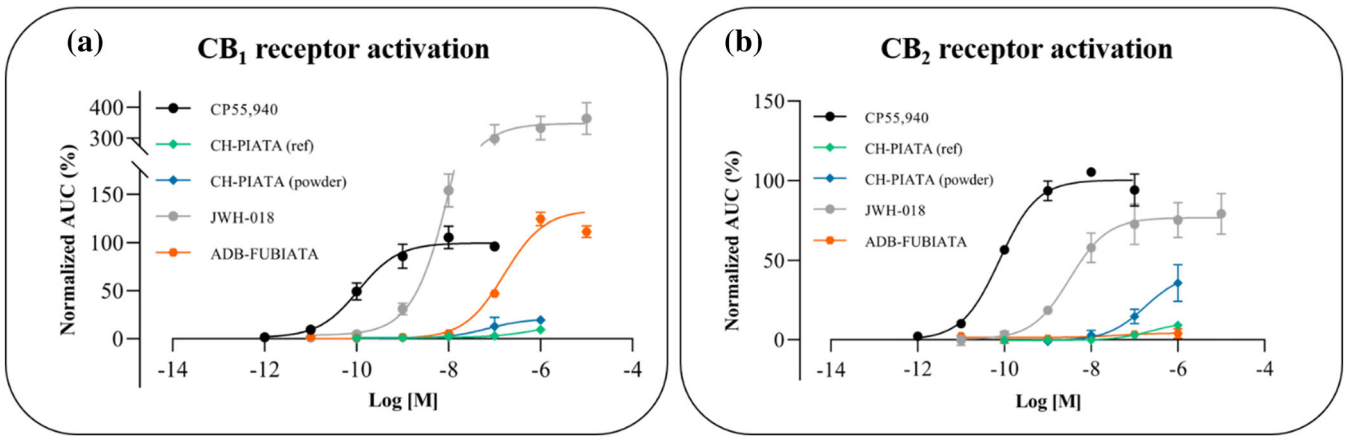

FIGURE 4 Concentration–response curves for the CH-PIATA reference standard and seized powder, alongside SCRA CP55,940 and JWH-018 at the CB_1 (panel a) and CB_2 (panel b) receptors. Data points represent the mean AUC value ± standard error of the mean (SEM) of minimally three independent experiments, run in duplicate. Note the difference in scaling of the y-axis.

TABLE 2 Potency (EC_{50}) and efficacy (E_{max}, relative to CP55,940) values obtained for the CH-PIATA reference standard and seized powder, as well as JWH-018.

	CB_1		CB_2	
	EC_{50} (nM) (95% CI)	E_{max} (%) (95% CI)	EC_{50} (nM) (95% CI)	E_{max} (%) (95% CI)
CH-PIATA (ref. stand.)	>690[a]	<10[b]	>259[a]	<10[b]
CH-PIATA (seized powder)	>71[a]	19[b]	>176[a]	36[b]
JWH-018	13.4 (6.11–30.7)	348 (311–387)	3.23 (1.14–9.21)	76.6 (67.1–86.5)
CP55,940	0.11 (0.05–0.26)	99.8 (89.4–111)	0.08 (0.05–0.13)	100 (93.6–107)

[a]EC_{50} values for the CH-PIATA reference standard could not be calculated accurately because saturation was not reached.
[b]Maximal activation observed at a concentration of 1 μM.

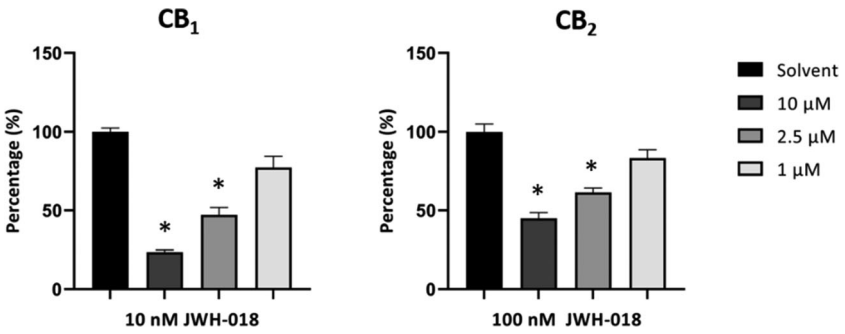

FIGURE 5 Activation of the CB_1 (panel a) and CB_2 (panel b) receptors by 10 nM (CB_1) and 100 nM (CB_2) of JWH-018 in cells pre-treated with solvent (black) or 10, 2.5, or 1 μM of CH-PIATA. Data are represented as % activation (compared with receptor activation of 10-nM JWH-018 in solvent-treated cells, set at 100%) ± SEM ($n = 3$). Bars assigned with an asterisk (*) are significantly different from solvent-treated controls ($p < 0.05$).

ADB-FUBIATA [orange] is plotted in Figure 4 alongside CH-PIATA).[50] Interestingly, here and in earlier reports, ADB-FUBIATA showed very distinct CB_1 and CB_2 receptor activation profiles, with a moderate CB_1 receptor activity but a complete lack of CB_2 activity.[22] This is in stark contrast with our results for CH-PIATA, demonstrating an equally low activity at both CB receptors. Given the absence of a pronounced receptor activation potential, the potential antagonistic behavior by CH-PIATA was also evaluated, as depicted in Figure 5. At both receptors, high concentrations (10, 2.5, and 1 μM) of CH-PIATA were found to be able to compete with lower concentrations of JWH-018 (10 nM at CB_1, 100 nM at CB_2) in a concentration dependent manner. As this indicates that CH-PIATA can block the receptor and inhibits cannabinoid signaling by JWH-018, it can be deduced that the low activation potential is not caused by an absence of receptor binding, similar to what was observed previously for ADB-FUBIATA.[22] Although interesting, investigating the true underlying cause for this phenomenon lies beyond the scope of this report. Obviously, as both the head and tail moiety differ between the two SCRAs, a further, in-depth comparison of their cannabinoid activity is not valid.

Additionally, a sample of a powder seized by Belgian customs was analyzed at both CB receptors alongside the reference standard. Maximal effects of 19% and 36% compared with CP55,940 were observed at the highest concentration of 1 μM at the CB_1 and CB_2 receptors, respectively (no plateau of maximal activation was reached). Based on the obtained concentration–response curves and estimated efficacy values, the seized powder exhibited a more pronounced receptor activation potential, which was most outspoken at the CB_2 receptor. As discussed above, the seized sample consisted of approximately 80% CH-PIATA together with several other SCRAs, which may have contributed to the discrepancy between the activation profiles of the reference standard and the sample. This finding also highlights the relevance of the use of activity-based bioassays to evaluate seized powders: they allow an appreciation of the overall activity contained within a sample, rather than solely the activity of a major component. Given the fact that there are large differences in the intrinsic receptor activation potential of distinct SCRAs (and NPS in general), this is relevant for a correct risk assessment of recreational SCRA preparations. For instance, a preparation may contain a large amount of a weakly active cannabinoid that is easily picked up using routine analytical techniques and a small amount of an ultrapotent, unidentified cannabinoid, which may be much more difficult to detect despite its major contribution to the total cannabinoid activity of the sample. Hence, an advantage of the activity-based approach is that it allows the assessment of the total cannabinoid activity of a product or preparation, from a receptor activation perspective, which is associated with the potential harm to the user upon consumption.

Although these assays are of value for screening and obtaining insights into the total cannabinoid activity contained in a seized product, there are some limitations that should be noted. For instance, activity-based bioassays cannot be used for identification and qualification of substances. Analytical confirmation of the contents of a preparation are therefore always essential. Of relevance here is that the potential (co-) occurrence of compounds with antagonistic properties (as is the case in the sample investigated here), may lead to a powder being mislabeled as "negative" for (active) cannabinoids in case of an absence of a rise in luminescence signal. Hence, due to the inherent ability of antagonists to block the receptor, receptor-based screening may fall short. Further testing, such as the antagonist

experiments performed in this study, can provide additional information. Of note, such preparations would likely be devoid of psychoactive effects (given the overall lack of CB_1 receptor activation potential) and hence would be less likely to be used by recreational drug users. Lastly, given the fact that these assays monitor a single pharmacological event (βarr2 recruitment), it cannot be fully ruled out that new compounds may preferentially result in alternative (non-βarr2) downstream intracellular pathways (e.g., biased agonists). However, at this point, no such substances have been identified.

4 | CONCLUSION

CH-PIATA is a newly emerged SCRA that circumvents the new Chinese SCRA analog controls through the addition of an extra methylene spacer in the linker moiety of the structure. Its detection in seized samples from Scotland and Belgium and in a blood sample in the United States demonstrates the international proliferation of this SCRA on the drug market. In vitro functional characterization of CH-PIATA demonstrated low efficacy and potency at the CB receptors, indicating it is unlikely to produce the desired psychoactive effects for users. Despite this fact, CH-PIATA has continued to be detected through the end of 2022. Therefore, clinical and forensic toxicologists are advised to add the CH-PIATA characteristic ions and metabolites, particularly M1 and M2, to their targeted and semi-targeted analytical methods. They should also remain vigilant to the emergence of other SCRAs with an acetamide linker and/or cyclohexyl head group that evade the Chinese SCRA ban, such as ADB-IATA (ADB-IACA) and CH-IATA (CH-IACA) which have already been notified to the EU Early Warning System.[41,51]

AUTHOR CONTRIBUTIONS

Conceptualization: Caitlyn Norman, Marie H. Deventer, Niamh Nic Daéid, Alex Krotulski, Christophe P. Stove. *Methodology*: Caitlyn Norman, Marie H. Deventer, Olivia Dremann, Robert Reid, Katleen Van Uytfanghe, Claude Guillou, Inge M. J. Vinckier, Alex Krotulski, Christophe P. Stove. *Data analysis*: Caitlyn Norman, Marie H. Deventer, Olivia Dremann, Robert Reid, Katleen Van Uytfanghe, Claude Guillou, Inge M. J. Vinckier, Alex Krotulski, Christophe P. Stove. *Writing—original draft*: Caitlyn Norman, Marie H. Deventer, Alex Krotulski. *Writing—review and editing*: All. *Supervision*: Caitlyn Norman, Niamh Nic Daéid, Alex Krotulski, Christophe P. Stove.

ACKNOWLEDGMENTS

MHD acknowledges funding from the Research Foundation Flanders (FWO; grant 1S54521N). We acknowledge Cayman Chemical for the gifting of the reference standard of CH-PIATA, used for the evaluation of the in vitro activity. Nick Verhavert is acknowledged for the practical assistance during his master's thesis. Dr. Fabiano Reniero and Margaret Holland from the JRC are acknowledged for their assistance during the NMR analyses. The Scottish-led part of the study was funded by the Scottish Prison Service (Procurement Reference 01865) and the Leverhulme Trust which funds the Leverhulme Research Centre for Forensic Science (grant number RC-2015-01). The United States portion of this project was supported by Arcadia University and the National Institute of Justice, Office of Justice Programs, US Department of Justice (Award Number 2020-DQ-BX-0007) awarded to the Center for Forensic Science Research and Education. The opinions, findings, and conclusions or recommendations expressed in this publication are those of the authors and do not necessarily represent the official position or policies of the U.S. Department of Justice.

CONFLICT OF INTEREST STATEMENT

The authors do not report any conflicts of interest.

ORCID

Caitlyn Norman https://orcid.org/0000-0003-2322-0367
Marie H. Deventer https://orcid.org/0000-0001-6667-2561
Katleen Van Uytfanghe https://orcid.org/0000-0001-8195-150X
Claude Guillou https://orcid.org/0000-0002-6210-3457
Inge M. J. Vinckier https://orcid.org/0000-0003-2394-3485
Niamh Nic Daéid https://orcid.org/0000-0002-9338-0887
Alex Krotulski https://orcid.org/0000-0003-1775-1882
Christophe P. Stove https://orcid.org/0000-0001-7126-348X

REFERENCES

1. European Monitoring Centre for Drugs and Drug Addiction (EMCDDA). *European Drug Report 2022: Trends and Developments*. Publications Office of the European Union; 2022. doi:10.2810/75644
2. Banister SD, Connor M. The chemistry and pharmacology of synthetic cannabinoid receptor agonists as new psychoactive substances: Origins. In: Maurer HH, Brandt SD, eds. *New Psychoactive Substances: Handbook of Experimental Pharmacology*. Vol.252. Springer International Publishing AG; 2018:165-190. doi:10.1007/164_2018_143
3. Potts AJ, Cano C, Thomas SHL, Hill SL. Synthetic cannabinoid receptor agonists: classification and nomenclature. *Clin Toxicol*. 2020;58(2):82-98. doi:10.1080/15563650.2019.1661425
4. Krishna Kumar K, Shalev-Benami M, Robertson MJ, et al. Structure of a signaling cannabinoid receptor 1-G protein complex. *Cell*. 2019;176(3):448-458. doi:10.1016/j.cell.2018.11.040
5. Hua T, Vemuri K, Pu M, et al. Crystal structure of the human cannabinoid receptor CB1. *Cell*. 2016;167(3):750-762. doi:10.1016/j.cell.2016.10.004
6. Li X, Hua T, Vemuri K, et al. Crystal structure of the human cannabinoid receptor CB2. *Cell*. 2019;176(3):459-467. doi:10.1016/j.cell.2018.12.011
7. Banister SD, Connor M. The chemistry and pharmacology of synthetic cannabinoid receptor agonists as new psychoactive substances: Evolution. In: Maurer HH, Brandt SD, eds. *New Psychoactive Substances: Handbook of Experimental Pharmacology*. Vol.252. Springer International Publishing AG; 2018:191-226. doi:10.1007/164_2018_144
8. Banister SD, Moir M, Stuart J, et al. Pharmacology of indole and indazole synthetic cannabinoid designer drugs AB-FUBINACA, ADB-FUBINACA, AB-PINACA, ADB-PINACA, 5F-AB-PINACA, 5F-ADB-PINACA, ADBICA, and 5F-ADBICA. *ACS Chem Neurosci*. 2015;7(9):1241-1254. doi:10.1021/acschemneuro.5b00112
9. Wouters E, Mogler L, Cannaert A, Auwärter V, Stove C. Functional evaluation of carboxy metabolites of synthetic cannabinoid receptor agonists featuring scaffolds based on L-valine or L-tert-leucine. *Drug Test Anal*. 2019;11(8):1183-1191. doi:10.1002/dta.2607

10. Manini AF, Krotulski AJ, Schimmel J, et al. Respiratory failure in confirmed synthetic cannabinoid overdose. *Clin Toxicol*. 2022;60(4):524-526. doi:10.1080/15563650.2021.1975734
11. Darke S, Banister S, Farrell M, Duflou J, Lappin J. 'Synthetic cannabis': a dangerous misnomer. *Int J Drug Policy*. 2021;98:103396. doi:10.1016/j.drugpo.2021.103396
12. Giorgetti A, Busardò FP, Tittarelli R, Auwärter V, Giorgetti R. Postmortem toxicology: a systematic review of death cases involving synthetic cannabinoid receptor agonists. *Front Psych*. 2020;11:464. doi:10.3389/fpsyt.2020.00464
13. European Monitoring Centre for Drugs and Drug Addiction (EMCDDA). *Fentanils and synthetic cannabinoids: driving greater complexity into the drug situation*. Publications Office of the European Union; 2018. doi:10.2810/603753
14. Raithelhuber M. @raithelhuber. "For all those interested in the #chemical details of the recent generic #legislation in #China on #Synthetic-Cannabinoids, now in English. @IUjvary @andcunningham @brycepardo @christophestove @unodc_lab." 2021. Accessed June 24, 2021. https://twitter.com/raithelhuber/status/1395062479827476481
15. Deventer MH, Van Uytfanghe K, Vinckier IMJ, Reniero F, Guillou C, Stove CP. Cannabinoid receptor activation potential of the next generation, generic ban evading OXIZID synthetic cannabinoid receptor agonists. *Drug Test Anal*. 2022;14(9):1565-1575. doi:10.1002/dta.3283
16. Norman C, Halter S, Haschimi B, et al. A transnational perspective on the evolution of the synthetic cannabinoid receptor agonists market: comparing prison and general populations. *Drug Test Anal*. 2021;13(4):841-852. doi:10.1002/dta.3002
17. Norman C, Walker G, McKirdy B, et al. Detection and quantitation of synthetic cannabinoid receptor agonists in infused papers from prisons in a constantly evolving illicit market. *Drug Test Anal*. 2020;12(4):538-554. doi:10.1002/dta.2767
18. Sachdev S, Vemuri K, Banister SD, et al. In vitro determination of the CB1 efficacy of illicit synthetic cannabinoids. *Br J Pharmacol*. 2019;176(24):4653-4665. doi:10.1111/bph.14829
19. Deventer MH, Norman C, Reid R, McKenzie C, Nic Daéid N, Stove CP. In vitro characterization of the pyrazole-carrying synthetic cannabinoid receptor agonist 5F-3,5-AB-PFUPPYCA and its structural analogs. *Forensic Sci Int*. 2023;343:111565. doi:10.1016/j.forsciint.2023.111565
20. Krotulski AJ, Farrell R, Roberson Z, Fogarty MF, Walton SE, Logan BK. *ADB-5Br-INACA*. Center for Forensic Science Research and Education; 2022. Accessed February 6, 2023. https://www.cfsre.org/images/monographs/ADB-5Br-INACA-051722-CFSRE-Chemistry-Report.pdf
21. Krotulski AJ, Farrell R, Schilde K, Fogarty MF, Walton SE, Logan BK. *MDMB-5Br-INACA*. Center for Forensic Science Research and Education; 2022. Accessed February 6, 2023. https://www.cfsre.org/images/monographs/MDMB-5Br-INACA-051722-CFSRE-Chemistry-Report.pdf
22. Deventer MH, Van Uytfanghe K, Vinckier IMJ, Reniero F, Guillou C, Stove CP. A new cannabinoid receptor 1 selective agonist evading the 2021 "China ban": ADB-FUBIATA. *Drug Test Anal*. 2022;14(9):1639-1644. doi:10.1002/dta.3285
23. Krotulski AJ, Farrell R, Schilde K, et al. *ADB-FUBIATA*. Center for Forensic Science Research and Education; 2022. Accessed November 10, 2022. https://www.cfsre.org/images/monographs/ADB-FUBIATA_111721_CFSRE_Chemistry_Report.pdf
24. European Monitoring Centre for Drugs and Drug Addiction (EMCDDA). EU Early Warning System Formal Notification. [Notification of CH-PIACA in Europe.] EU-EWS-RCS-FN-2022-0008. 2022.
25. Pasin D, Nedahl M, Mollerup CB, Tortzen C, Reitzel LA, Dalsgaard PW. Identification of the synthetic cannabinoid-type new psychoactive substance, CH-PIACA, in seized material. *Drug Test Anal*. 2022;14(9):1645-1651. doi:10.1002/dta.3333
26. Krotulski AJ, Farrell R, Mohaupt A, Fogarty MF, Walton SE, Logan BK. *CH-PIATA*. Center for Forensic Science Research and Education; 2022. Accessed February 6, 2023. https://www.cfsre.org/images/monographs/CH-PIATA-042922-CFSRE-Chemistry-Report.pdf
27. National Forensic Laboratory Information System (NFLIS). Drug Snapshot June 2022. 2022. Accessed February 6, 2023. https://www.nflis.deadiversion.usdoj.gov/publicationsRedesign.xhtml
28. Watanabe S, Kuzhiumparambil U, Nguyen MA, Cameron J, Fu S. Metabolic profile of synthetic cannabinoids 5F-PB-22, PB-22, XLR-11 and UR-144 by Cunninghamella elegans. *AAPS J*. 2017;19(4):1148-1162. doi:10.1208/s12248-017-0078-4
29. Brandon AM, Antonides LH, Riley J, et al. A systematic study of the in vitro pharmacokinetics and estimated human in vivo clearance of indole and indazole-3-carboxamide synthetic cannabinoid receptor agonists detected on the illicit drug market. *Molecules*. 2021;26(5):1396-1422. doi:10.3390/molecules26051396
30. Diao X, Huestis MA. New synthetic cannabinoids metabolism and strategies to best identify optimal marker metabolites. *Front Chem*. 2019;7:109. doi:10.3389/fchem.2019.00109
31. Cannaert A, Storme J, Franz F, Auwärter V, Stove CP. Detection and activity profiling of synthetic cannabinoids and their metabolites with a newly developed bioassay. *Anal Chem*. 2016;88(23):11476-11485. doi:10.1021/acs.analchem.6b02600
32. Cannaert A, Franz F, Auwärter V, Stove CP. Activity-based detection of consumption of synthetic cannabinoids in authentic urine samples using a stable cannabinoid reporter system. *Anal Chem*. 2017;89(17):9527-9536. doi:10.1021/acs.analchem.7b02552
33. Cannaert A, Storme J, Hess C, Auwärter V, Wille SMR, Stove CP. Activity-based detection of cannabinoids in serum and plasma samples. *Clin Chem*. 2018;64(6):918-926. doi:10.1373/clinchem.2017.285361
34. Antonides LH, Cannaert A, Norman C, et al. Shape matters: the application of activity-based in vitro bioassays and chiral profiling to the pharmacological evaluation of synthetic cannabinoid receptor agonists in drug-infused papers seized in prisons. *Drug Test Anal*. 2020;13(3):628-643. doi:10.1002/dta.2965
35. Kronstrand R, Norman C, Vikingsson S, et al. The metabolism of the synthetic cannabinoids ADB-BUTINACA and ADB-4en-PINACA and their detection in forensic toxicology casework and infused papers seized in prisons. *Drug Test Anal*. 2022;14(4):634-652. doi:10.1002/dta.3203
36. Thoren KL, Colby JM, Shugarts SB, Wu AHB, Lynch KL. Comparison of information-dependent acquisition on a tandem quadrupole TOF vs a triple quadrupole linear ion trap mass spectrometer for broad-spectrum drug screening. *Clin Chem*. 2016;62(1):170-178. doi:10.1373/clinchem.2015.241315
37. Blanckaert P, van Cannaert A, Uytfanghe K, et al. Report on a novel emerging class of highly potent benzimidazole NPS opioids: chemical and in vitro functional characterization of isotonitazene. *Drug Test Anal*. 2020;12(4):422-430. doi:10.1002/dta.2738
38. Lobo Vicente J, Chassaigne H, Holland MV, et al. Systematic analytical characterization of new psychoactive substances: a case study. *Forensic Sci Int*. 2016;265:107-115. doi:10.1016/j.forsciint.2016.01.024
39. Grafinger KE, Cannaert A, Ametovski A, et al. Systematic evaluation of a panel of 30 synthetic cannabinoid receptor agonists structurally related to MMB-4en-PICA, MDMB-4en-PINACA, ADB-4en-PINACA, and MMB-4CN-BUTINACA using a combination of binding and different CB1 receptor activation assays—part II: structure activity relationship assessment via a β-arrestin recruitment assay. *Drug Test Anal*. 2021;13(7):1402-1411. doi:10.1002/dta.3035
40. Cannaert A, Sparkes E, Pike E, et al. Synthesis and in vitro cannabinoid receptor 1 activity of recently detected synthetic cannabinoids 4F-MDMB-BICA, 5F-MPP-PICA, MMB-4en-PICA, CUMYL-CBMICA, ADB-BINACA, APP-BINACA, 4F-MDMB-BINACA, MDMB-4en-

PINACA, A-CHMINACA, 5F-AB-P7AICA, 5F-MDMB-P7AICA, and 5F-AP7AICA. *ACS Chem Nerosci*. 2020;11(24):4434-4446. doi:10.1021/acschemneuro.0c00644
41. European Monitoring Centre for Drugs and Drug Addiction (EMCDDA). EU Early Warning System Formal Notification. [Notification of CH-IACA in Europe]. EU-EWS-RCS-FN-2022-0027. 2022.
42. Dahm P, Thomas A, Rothschild MA, Thevis M, Mercer-Chalmers-Bender K. Phase I-metabolism studies of the synthetic cannabinoids PX-1 and PX-2 using three different in vitro models. *Forensic Toxicol*. 2022;40(2):244-262. doi:10.1007/s11419-021-00606-6
43. Watanabe S, Vikingsson S, Åstrand A, Gréen H, Kronstrand R. Biotransformation of the new synthetic cannabinoid with an alkene, MDMB-4en-PINACA, by human hepatocytes, human liver microsomes, and human urine and blood. *AAPS J*. 2020;22(1):13. doi:10.1208/s12248-019-0381-3
44. Longworth M, Connor M, Banister SD, Kassiou M. Synthesis and pharmacological profiling of the metabolites of synthetic cannabinoid drugs APICA, STS-135, ADB-PINACA, and 5F-ADB-PINACA. *ACS Chem Nerosci*. 2017;8(8):1673-1680. doi:10.1021/acschemneuro.7b00116
45. Kevin RC, Lefever TW, Snyder RW, et al. In vitro and in vivo pharmacokinetics and metabolism of synthetic cannabinoids CUMYL-PICA and 5F-CUMYL-PICA. *Forensic Toxicol*. 2017;35(2):333-347. doi:10.1007/s11419-017-0361-1
46. Truver MT, Watanabe S, Åstrand A, et al. 5F-MDMB-PICA metabolite identification and cannabinoid receptor activity. *Drug Test Anal*. 2020;12(1):127-135. doi:10.1002/dta.2688
47. Sia CH, Wang Z, Goh EML, et al. Urinary metabolite biomarkers for the detection of synthetic cannabinoid ADB-BUTINACA abuse. *Clin Chem*. 2021;67(11):1534-1544. doi:10.1093/clinchem/hvab134
48. Kavanagh P, Pechnikov A, Nikolaev I, Dowling G, Kolosova M, Grigoryev A. Detection of ADB-BUTINACA metabolites in human urine, blood, kidney and liver. *J Anal Toxicol*. 2022;46(6):641-650. doi:10.1093/jat/bkab088
49. Ozturk YE, Yeter O. In vitro phase I metabolism of the recently emerged synthetic MDMB-4en-PINACA and its detection in human urine samples. *J Anal Toxicol*. 2020;44(9):1012-1026. doi:10.1093/jat/bkaa017
50. Liu C-M, Hua Z-D, Jia W, Li T. Identification of AD-18, 5F-MDA-19, and pentyl MDA-19 in seized materials after the class-wide ban of synthetic cannabinoids in China. *Drug Test Anal*. 2022;14(2):307-316. doi:10.1002/dta.3185
51. European Monitoring Centre for Drugs and Drug Addiction (EMCDDA). EU Early Warning System Formal Notification. [Notification of ADB-IATA in Europe]. EU-EWS-RCS-FN-2022-0004. 2022.

SUPPORTING INFORMATION

Additional supporting information can be found online in the Supporting Information section at the end of this article.

How to cite this article: Norman C, Deventer MH, Dremann O, et al. In vitro cannabinoid receptor activity, metabolism, and detection in seized samples of CH-PIATA, a new indole-3-acetamide synthetic cannabinoid. *Drug Test Anal*. 2024;16(4):380-391. doi:10.1002/dta.3555